PROTEINS: Structure, Function, and Genetics 15:235–251 (1993)

βVI Turns in Peptides and Proteins: A Model Peptide Mimicry

Gerhard Müller, Marion Gurrath, Michael Kurz, and Horst Kessler
Organisch Chemisches Institut, Technische Universität München, W-8046 Garching, Federal Republic of Germany

ABSTRACT **To investigate the role of proline in defining β turn conformations within cyclic hexa- and pentapeptides we synthesized and determined the conformations of a series of L- and D-proline-containing peptides by means of 2D NMR spectroscopy and restrained molecular dynamics simulations. Due to *cis/trans* isomerism the L-proline peptides adopt at least two different conformations that are analyzed and compared to the structures of the corresponding D-proline peptides. The *cis* conformations of the compounds *cyclo*(-Pro-Ala-Ala-Pro-Ala-Ala-), *cyclo*(-Arg-Gly-Asp-Phe-Pro-Gly-), *cyclo*(-Arg-Gly-Asp-Phe-Pro-Ala-), *cyclo*(-Pro-Ala-Ala-Ala-Ala-), and *cyclo*(-Pro-Ala-Pro-Ala-Ala-) form uncommon βVI turns that mimic the turn geometries found in crystallographically refined protein structures at such a detailed level that even preferred side chain orientations are reproduced. The ratios of the *cis/trans* isomers are analyzed in terms of the steric demand of the proline-following residue. The conformational details derived from this study illustrate the importance of the examination of small model compounds derived from protein loop regions, especially if bioactive recognition sequences, such as RGD (Arg-Gly-Asp), are incorporated.** © 1993 Wiley-Liss, Inc.

Key words: conformational analysis, 2D NMR spectroscopy, restrained molecular dynamics, RGD peptides, proline, *cis/trans* isomerism, peptide templates

INTRODUCTION

One of the most challenging efforts in molecular biology is to understand biological processes in terms of the chemistry and physics of the participating biopolymers on a structural level. The three-dimensional structure of, e.g., proteins, and therefore a wide variety of biological functions are controlled by the variation of only a few structural principles,[1–4] i.e., helices, β sheets, and hairpins. The β hairpin is a common feature of protein structure by changing the polypeptide chain direction by nearly 180°.[5,6] The essential conformational element of hairpins is the reverse turn.

Venkatachalam in 1968 identified a certain subset of reverse turns, the four residue β turn, where a hydrogen bond is formed between the main chain NH of the fourth amino acid (i + 3) and CO of the first residue (i) (Fig. 1).[7]

A more general definition of β turns originates in 1973 from Lewis, who stated that the distance between the C^{α}_i and C^{α}_{i+3} should be smaller than 7 Å and the four involved residues may not be part of a helix.[8] The most widely used classification was given by Richardson in 1981,[4] based on the values of the peptide backbone dihedral angles φ, ψ, and ω, defining six different classes of β turns: βI, βI′, βII, βII′, βVIa, and βVIb.[4,9,10] These turns are differentiated by the backbone conformations of the i + 1 and i + 2 residues (Table I).

Proline has the highest specific positional preference of the residues located in reverse turns[11] and severely constrains the backbone when compared to the other amino acids, since the ring closure restricts φ to −60°. A further property which is almost unique to proline is the formation of *cis* and *trans* peptide bonds (ω_{i-1} relative to Pro_i).[12] With a *trans* peptide bond, proline mainly occupies the i + 1 position of type I or type II β turns maintaining a φ angle of −60° (Table I). A *cis* proline occupies the i + 2 position of a type VI or *cis* proline turn. Two distinct type VI turns are found differing in the ψ angle of the proline: βVIa with ψ near 0° and a hydrogen bond from NH_{i+3} to CO_i, and a βVIb turn with ψ around 150°, shifting the following amide bond so that no turn-stabilizing hydrogen bond is formed. Proline in βVI turns causes important structural implications on the conformation of the preceding residue, which is almost exclusively in an extended conformation and shows preferences in side chain orientation. Taking these structural implications of proline into account it was a challenging task for us to design cyclic peptides containing L-Pro and D-Pro residues in order to study their conformational characteristics by means of 2D NMR spectroscopy[13] and refinement by *restrained* molecular mechanics sim-

Received February 24, 1992; revision accepted July 20, 1992.
Address reprint requests to Dr. Horst Kessler, Organisch Chemisches Institut, Technische Universität München, Lichtenbergstrasse 4, W-8046 Garching, Federal Republic of Germany.

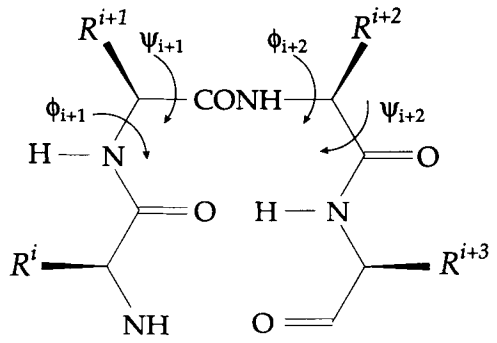

Fig. 1. Nomenclature of residues and main chain torsions within common β turns.

TABLE I. Main Chain Torsion Values for Regular Polypeptide Conformations[4,9,10]

Conformation	ϕ_{i+1}	ψ_{i+1}	ϕ_{i+2}	ψ_{i+2}
βI turn	−60	−30	−90	0
βI′ turn	60	30	90	0
βII turn	−60	120	80	0
βII′ turn	60	−120	−80	0
βVIa turn	−60	120	−90	0
βVIb turn	−120	120	−60	150*
α helix	−57	−47	−57	−47
3_{10} helix	−60	−30	−60	−30
Polyproline II	−78	149	−78	149

*A contradiction for the ψ_{i+2} dihedral angle value is found in the literature. In refs. 4 and 9 ψ_{i+2} is set to 0°, while in refs. 10 and 58, and in βVIb containing crystallographically refined protein structures ψ_{i+2} is found at values around 150°.

ulations. The compounds being discussed first, consisting only of the amino acids proline, alanine, and glycine, have been designed to create structural templates in a conformational controlled manner. The restriction in conformational freedom by backbone cyclization and the incorporation of proline and D-residues increases the probability that experimental conformational analysis will identify predominant solution conformers.[14] These conformers of the model peptides can serve as scaffolds for orienting essential functional groups by changing selected Ala or Gly residues to the desired functionalized amino acids. In this way, the orientation of a potential pharmacophore can be controlled by choosing appropriate positions for biological relevant sequences within the model peptide structures. So the design of tailor-made bioactive peptides becomes possible.[15]

We applied that rational design principle on the bioactive Arg-Gly-Asp (RGD) sequence, a universal cell recognition site in adhesive proteins, mediating a wide range of cell adhesion phenomena.[16] Positioning of that tripeptide sequence in different manners within common underlying templates led to active and selective tumor cell adhesion antagonists.[17] A similar approach was followed by Kopple et al. only recently; they introduced a D-Pro-L-Pro sequence into RGD containing cyclic hexapeptides to define and fix the arrangement of a two-β turn backbone.[18]

We will focus on a structure elucidation of peptides containing proline in either the all-*trans* configuration in the $i + 1$ position of βI and βII turns or in the *cis* configuration occupying the $i + 2$ position of βVIa and βVIb turns. The effect of ring size of the cyclic model peptide systems and of inversion of L-Pro to D-Pro will be discussed in terms of conformational homogeneity. The refined conformations will be compared to conformational studies of sequentially related peptides from the literature. Additionally, a correlation of the steric demand of the amino acid following proline to the ratio of the *cis* and *trans* conformers will be given. Finally we will propose an explanation for the determined sequence preference of hydrophobic and aromatic residues in the position preceding a *cis* proline in type VI β turns, based on the NMR-derived analysis of side chain orientations and the discussion of chemical shift values. The results obtained will be compared with βVI turn conformations in proteins, based on crystallographically refined structures taken from the Brookhaven Protein Data Bank.

EXPERIMENTAL PROCEDURE

Synthesis

The peptides were synthesized by stepwise solid phase peptide synthesis using either chloromethylated polystyrene, *o*-chlorotritylchloride resin, or Sasrin resin following either a Boc (*tert*-butyloxycarbonyl) strategy in DCM (dichloromethane) or a Fmoc (9-fluorenylmethoxycarbonyl) strategy in DMF (*N,N*-dimethylformamide). In the coupling procedure DCC/HOBt (1,3-dicyclohexylcarbodiimide/1-hydroxybenzotriazole) or TBTU/HOBt (2-(1*H*-benzotriazol-1-yl)-1,1,3,3-tetramethyluronium tetrafluoroborate) has been applied in combination with DIPEA (*N,N*-diisopropylethylamine) in NMP (1-methyl-2-pyrrolidinone). Cyclization was performed by the azide method under high dilution in DMF. The peptides were purified by reversed-phase high-performance liquid chromatography (HPLC) and characterized by fast atom bombardment mass spectrometry (FAB-MS) and amino acid analysis.

NMR Spectroscopy

All samples for NMR spectroscopy were prepared at 10–20 mM peptide concentration in DMSO-d_6 (dimethyl sulfoxide) and were degased. The spectra were recorded on Bruker AC 250, AMX 500, and AMX 600 spectrometers and the data processed on Bruker X32 computers with UXNMR software.

The assignment of the proton resonances was performed using a set of 1D and 2D NMR spectra: double-quantum filtered correlated spectroscopy

(DQF-COSY)[19] and total correlation spectroscopy (TOCSY)[20,21] with 20 and 80 ms spin lock period. The sequential assignment was based on nuclear Overhauser enhancement and exchange spectroscopy (NOESY)[22,23] and rotating frame nuclear Overhauser effect spectroscopy (ROESY)[24–26] spectra and heteronuclear multiple bond correlation (HMBC) experiments using a 270° Gaussian pulse for selective excitation of the ^{13}C carbonyl resonances (HMBCS).[27,28] Diastereotopic assignment of prochiral protons and analysis of side chain conformations were achieved by HMBCS in combination with homonuclear coupling constants from exclusive COSY (E.COSY) spectra.[29] Assignment of ^{13}C resonances was carried out with heteronuclear multiple quantum coherence (HMQC)[30] and HMQC with TOCSY transfer.[31] Heteronuclear long-range couplings were detected with HMBC and with HETLOC experiments.[32,33]

The temperature dependence of the amide signals was studied following the NH resonances through a series of 1D spectra taken at several temperatures within the range of 300–325 K. The ROEs and NOEs were translated into interproton distances after calibration by an r^{-6} correlation of the cross-peak intensities using the two-spin approximation. Before calibration, the ROEs were corrected for the offset of the spin lock frequence.[34] The obtained distances and temperature coefficients served as input for restrained molecular mechanics simulations.

Molecular Mechanics Simulations

All energy minimizations (EM) and molecular dynamics (MD) simulations were performed using the programs of the Groningen Molecular Simulation software package (GROMOS)[35,36] on Silicon Graphics 4D/25TG, 4D/70GTB, and 4D/240SX computers using the program INSIGHT (BIOSYM)[37] for interactive modeling and graphic display. For numerical integration of the equation of motion in MD simulations the Verlet algorithm was used. To allow an integration time step of 2 fs all bond lengths were constrained by applying the SHAKE algorithm.[38] The simulations were carried out in vacuum with a relative dielectric permittivity of 1 *and* in a specially parameterized DMSO solvent box.[39] To overcome in vacuo derived conformational distortions due to overemphasized electrostatic interactions the charges of the NH charge groups were scaled down for all vacuum simulations according to the measured temperature coefficients of the NH resonances.[40] Nevertheless, when simulating peptides with charged side chains (Arg, Asp) it is much better to treat the solvent environment explicitly. The velocities given to the atoms initially were taken from a Maxwellian distribution for the desired temperature.

Restrained MD in in vacuo and in the same solvent in which the NMR experiments were done was performed, using the interproton distance information in the potential energy function with a harmonic potential scaled by a force constant k_{NOE}. Starting with a manually constructed structure, EM was carried out to remove any strain from model building. An MD simulation was run in vacuum at 1000 K for 2 ps, 500 K for 3 ps, and 300 K for 5 ps with k_{NOE} = 4000 kJ mol^{-1} nm^{-2}. This high temperature run was used to create a starting conformation which agrees with the experimental parameters for an in vacuo simulation (90 ps) *and* a simulation in a DMSO solvent box (150 ps), applying periodic boundary conditions. For the in vacuo calculations, the first 30 ps were used to equilibrate the system and the following 60 ps served for analysis. The solvent simulation started with the in vacuo derived conformations by soaking the peptide in a truncated octahedron-like box with a box length of approximately 3.5 nm containing about 150 solvent molecules. That system was subsequently relaxed by EM and the MD simulation was started at 300 K for 70 ps with k_{NOE} = 1000 kJ mol^{-1} nm^{-2}, the next 30 ps with k_{NOE} = 500 kJ mol^{-1} nm^{-2}, and the last 50 ps of the 150-ps trajectory without any restraints. The free dynamics simulation ensures that the conformation obtained after 100 ps of restrained MD is a stable, low-energy conformation. The complete trajectory covers 100 ps of restrained MD and 50 ps of free dynamics, which means 75000 integration steps for each atom in the solvent box. The structures given in Figures 3, 4, 5 and 7 and described in Tables III and VI are obtained by averaging over the last 60 ps of restrained MD and energy minimization.

RESULTS AND DISCUSSION

All peptides investigated contain a minimal sequential element, Xaa-L,D-Pro-Yaa, where the Xaa-L-Pro peptide bond is either *cis* or *trans*, Xaa is a side chain bearing residue (Ala, Phe), and Yaa is either Gly or Ala. The L-Pro peptides are found in at least two distinct conformations due to *cis/trans* isomerism around the Xaa–Pro peptide bond. This finding is based on the fact that each of these peptides shows two different sets of resonances in the ^1H NMR spectrum. The corresponding residues in either the *cis* or *trans* isomer can be identified by exchange peaks between their proton resonances in the 2D ROESY spectrum which is illustrated for c(RGDFPA) in Figure 2. If the minor isomer is populated by more than approximately 10%, it is possible to analyze the conformations of both conformers, which will be demonstrated here for *cyclo*(-Pro^1-Ala^2-Ala^3-Pro^4-Ala^5-Ala^6-) [c(PAAPAA)], *cyclo*(-Arg^1-Gly^2-Asp^3-Phe^4-Pro^5-Gly^6-) [c(RGDFPG)] and *cyclo*(-Arg^1-Gly^2-Asp^3-Phe^4-Pro^5-Ala^6-) [c(RGDFPA)].

The resonances of the *cis* isomer are easily identified by a difference in the proline C^β and C^γ shift

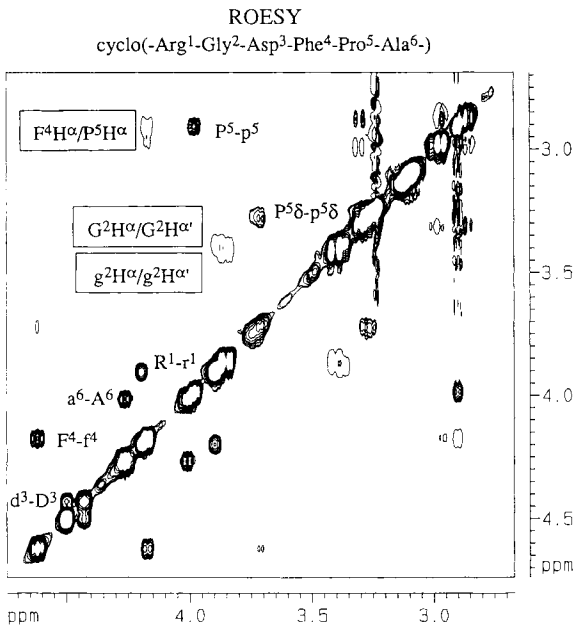

Fig. 2. The H^{α}/H^{α} region of a 600 MHz ROESY spectrum of c(RGDFPA) in DMSO-d_6 measured at 300 K. The spectrum was recorded with a mixing time of 180 ms and a spin lock power of 3 kHz. The exchange peaks correlating the H^{α} resonances in the *cis* and *trans* peptides and the cross peak, indicating the short Phe^4H^{α}, Pro^5H^{α} distance in the *cis* conformation are illustrated. Positive peaks (diagonal and exchange peaks) are plotted with 8 levels, negative peaks with 2 levels.

values of about 10 ppm, with $\delta C^{\beta} \approx 31$ ppm and $\delta C^{\gamma} \approx 22$ ppm, respectively.[12,14] In the *trans* conformation the resonances are around 28.5 ppm for C^{β} and around 25.0 ppm for C^{γ}. The chemical shifts of the C^{β} and C^{γ} resonances of both, the *cis* and *trans* isomers are given in Table II.

A further proof of a *cis* peptide bond is the short H^{α}–H^{α} distance of the adjacent amino acids, indicated by an intensive cross peak between the H^{α} resonances in the NOESY or ROESY spectra, yielding a distance after calibration of approximately 200 pm (Fig. 2).

βVIa Turn Peptides

The conformation of the C_2 symmetric model compound c(PAAPAA), which is the smallest cyclic peptide adopting a βVIa,βVIa conformation with side chain bearing residues, will serve as a representative of βVIa turn containing peptides. It is an ideal prototypic model for studying the uncommon type VIa β turn motif in a minimal peptide environment. The peptide adopts three different conformations in DMSO, as detected in the ^1H NMR spectrum. The ratios are 49:28:23 for the all-*trans*, two-*cis* and an asymmetric conformation. The all-*trans* conformation forms a two β turn arrangement, in which Pro^1/Pro^4 occupy the $i + 1$ positions in a nearly perfect C_2 symmetric structure (Fig. 3, top).

This particular turn arrangement is clearly supported by the temperature coefficients of the amide resonances of Ala^3/Ala^6 (0.00 ppb/K) and Ala^2/Ala^5 (−4.5 ppb/K). These gradients indicate that Ala^3NH/Ala^6NH are shielded (involved in internal hydrogen bonds), whereas Ala^2NH/Ala^5NH are exposed to the surrounding solvent. For the all-*trans* conformation 18 distance constraints were used for the restrained MD simulations, which are fulfilled in the averaged and minimized structure in Figure 3 (top) with an average restraint violation of 13 pm. The analysis of the hydrogen bond pattern monitored over the simulation confirms this conformation: the Ala^3NH/Ala^6CO and Ala^6NH/Ala^3CO hydrogen bonds are observed for 91 and 84% of the trajectory, respectively. The evaluated backbone dihedrals averaged over 60 ps of in vacuo MD simulations are in accordance with a βII,βII turn structure for the peptide, as shown in Table III.

The predominant βII,βII turn conformation is clearly supported by two experimentally derived interproton distances between Ala^2NH and Pro^1H^{α} (Ala^5NH and Pro^4H^{α}) with 223 pm and between Ala^2NH and Ala^2H^{α} (Ala^5NH and Ala^5H^{α}) with 238 pm. In case of a significant βI–βII conformational equilibrium,[41,42] these two distances would be increased. For a βI turn the Ala^2NH-Pro^1H^{α} (Ala^5NH-Pro^4H^{α}) and the Ala^2NH-Ala^2H^{α} (Ala^5NH-Ala^5H^{α}) distances are around 360 and 305 pm, respectively, which would not fit our experimental findings. It turned out that the $Xaa^{i+2}NH$-$Xaa^{i+2}H^{\beta}$ NOEs yield increased interproton distances when compared to a βII turn and can therefore be used as an indication for a βI–βII interconversion. In the all-*trans* conformation of c(PAAPAA) this particular correlation involves the methyl group of Ala^2 (Ala^5) and due to the commonly used pseudo-atom correction[35] for methyl groups this distance is not as evident as interproton distances between diastereotopically assigned β protons. However, the βII,βII turn structure for the all-*trans* conformation is in agreement with a structural elucidation of the cyclic hexapeptide *cyclo*(-Pro-Ser-Gly-Pro-Ser-Gly-).[43] This peptide also undergoes *cis*/*trans* isomerism and the all-*trans* conformation is found in a βII,βII turn structure, proline occupying the $i + 1$ position.[43] Usually in cyclic hexapeptides proline is found in the $i + 1$ position of a type II β turn only in Pro-Gly and Pro-D-Xaa sequences as was demonstrated for a series of C_2 symmetric cyclic hexapeptides by NMR investigations and X-ray analysis. These peptides follow a sequence pattern *cyclo*(-Pro-Xaa-Yaa-)$_2$ with either Xaa = Gly and Yaa = Gly,[44,45] Ser,[46] Val,[47] Phe[48] or Xaa = D-Ala, D-Phe and Yaa = Gly,[47–50] Ala,[51,52] Orn, [51] His,[51] Phe,[52] D-Ala,[48] D-Phe.[48]

The second conformer populated by 28% contains two Ala-Pro *cis* peptide bonds, supported by strong ROEs between $Ala^3H^{\alpha}/Ala^6H^{\alpha}$ and $Pro^4H^{\alpha}/Pro^1H^{\alpha}$

TABLE II. The Chemical Shift Values of the C^{β} and C^{γ} Atoms of the Proline Residues*

Peptides	Residues	δC^{β}	δC^{γ}	Δ	Configuration
c(PAAPAA)	Pro^1/Pro^4	28.5	25.6	2.9	*trans*
	Pro^1/Pro^4	31.2	21.8	9.4	*cis*
c(*P*AA*P*AA)	D-Pro^1/D-Pro^4	28.3	24.8	3.5	*trans*
c(RGDFPG)	Pro^5	28.2	25.4	2.8	*trans*
	Pro^5	30.5	21.6	8.9	*cis*
c(RGDFPA)	Pro^5	28.7	25.2	3.5	*trans*
	Pro^5	30.7	21.7	9.0	*cis*
c(PAAAA)	Pro^1	31.5	22.1	9.4	*cis*
c(PAPAA)	Pro^1	31.2	21.5	9.8	*cis*
	Pro^3	31.5	22.4	9.1	*cis*

*Values are given in ppm relative to DMSO set to 39.5 ppm. In the one-letter amino acid code D-residues are printed in italics.

defining a distance in the range of 200 pm. The ^{13}C resonances of Pro C^{β} and C^{γ} confirm the preceding *cis* peptide bond with δC^{β} = 31.2 ppm and δC^{γ} = 21.8 ppm (Table II). Surprisingly, the temperature coefficients of the NH resonances of Ala^2/Ala^5 and Ala^3/Ala^6 are −6.5 and −2.5 ppb/K, respectively, indicating no intramolecular hydrogen bond. However, a characteristic NOE (distance 260 pm) counting for the βVIa turn is caused by the spatial proximity of NH_{i+3} (Ala^2/Ala^5) and H^{α}_{i+1} (Ala^6/Ala^3). All distance constraints are fulfilled with an average restraint violation of 10 pm and coincide with the structure shown in Figure 3 (bottom). The peptide again shows the C_2 symmetry with a βVIa,βVIa turn arrangement, in which both proline residues are located in i + 2 position and, therefore, the complete sequence has been shifted clockwise by one position when compared to the turn arrangement of the peptide in the all-*trans* conformation. The averaged values of the main chain torsions are in agreement with a type VIa β turn (Table III). In addition the hydrogen bonds between Ala^2NH and Ala^5CO and between Ala^5NH and Ala^2CO are populated by only 18%, in agreement with the experimentally determined high (−6.5 ppb/K) temperature gradients. The reason for the low population of these hydrogen bonds during the simulation is a kink in the molecule along the line between Ala^2C^{α}-Ala^5C^{α}. This kink allows two additional hydrogen bonds to form on the exterior of the molecule, forming two inverse γ turns with Ala^2 and Ala^5 in their central i + 1 positions (Fig. 3, bottom). In in vacuo simulations these γ turns are often observed at the exterior of molecules and are due to overemphasized electrostatic interactions.[53] However, taking the low temperature coefficients of Ala^3NH/Ala^6NH into account, these γ_i turns are not vacuum-derived artifacts. To prove this assumption we additionally performed restrained and free MD simulations in a DMSO solvent box consisting of 304 DMSO molecules with a box length of 4.17 nm applying periodic boundary conditions. The averaged and minimized structure after 100 ps simulation is nearly identical to the in vacuo derived conformation depicted in Figure 3 (bottom), supported by a rms deviation of 0.78 Å for superimposing all atoms. The dihedral angle values averaged over the 100 ps solvent simulation are given in Table III. The average distance restraint violation could be improved to 8 pm. The experimentally derived temperature gradients as well as the agreement with the distance constraints in in vacuo and in solvent simulations account for the γ_i turn. The orientations of the preceding and following amide bonds of Ala^2/Ala^5 are twisted out of the ring plane which explains the deviation of ψ_{i+2} of both βVIa turn residues from the ideal values (Pro^1, Pro^4: ψ = −24°, −27°; ideal value: 0°) (Table IV). For the βVIa turn stabilizing hydrogen bonds, the bond angle, Θ_{DHA}, is decreased from an ideal value near linearity (180°) to 133°, and the donor–acceptor distance is larger.

There are several investigations of sequentially and conformationally related cyclic hexapeptides in the literature that have been analyzed by NMR spectroscopy and X-ray analysis. For example *cyclo*(-Pro-Gly-Ser-Pro-Gly-Ser-)[46] adopts a C_2 symmetric two-*cis* conformation in DMSO, populated by 80%. A more closely related peptide, *cyclo*(-Pro-D-Ala-Ala-Pro-D-Ala-Ala-), was analyzed by evaluation of $^3J_{NH,H\alpha}$ vicinal coupling constants, temperature coefficients of NH resonances, and proton exchange studies[51] and adopts a C_2 symmetric all-*trans* structure with Pro in the i + 1 position of a β turn and a further C_2 symmetric two-*cis* conformation with two βVIb turns, proline occupying the i + 2 positions. Even an X-ray structure of *cyclo*(-Pro-D-Ala-Phe-Pro-D-Ala-Phe-) was published in 1984 with two slightly different molecules in the asymmetric unit, both with two Phe-Pro *cis* peptide bonds.[54] Again, both C_2 symmetric conformations (A and B) match the backbone dihedral angles of a βVIb,βVIb conformation. For molecule A the backbone torsion values are ϕ_{i+1} = −153°, ψ_{i+1} = 133°, ϕ_{i+2} = −83°, ψ_{i+2} = 157°, ϕ'_{i+1} = −169°, ψ'_{i+1} = 134°, ϕ'_{i+2} = −70°, ψ'_{i+2} = 165′; for molecule B the values are ϕ_{i+1} = −149°, ψ_{i+1} = 143°, ϕ_{i+2} = −71°, ψ_{i+2} = 174°, ϕ'_{i+1} = −163°, ψ'_{i+1} = 140°, ϕ'_{i+2} = −63°, ψ'_{i+2} = −179°.[54] It is remarkable

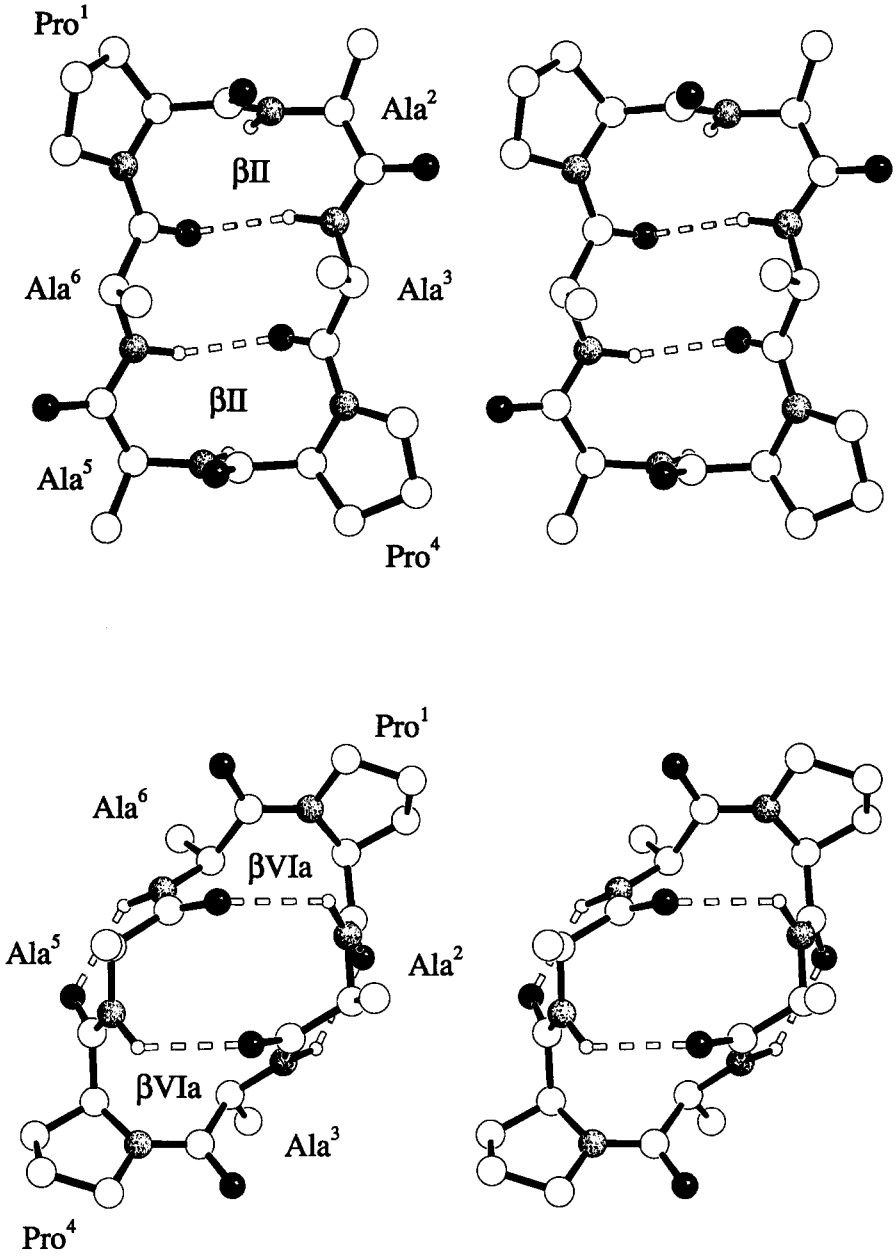

Fig. 3. Stereoplot of c(PAAPAA) in the all-*trans* (**top**) and two-*cis* (**bottom**) conformation. Oxygen atoms are depicted as filled balls, nitrogen atoms stippled, carbon atoms and hydrogen atoms are shown as plain balls. Hydrogen bonds are indicated as broken bonds.

that c(PAAPAA) clearly favors a βVIa turn geometry in the two-*cis* conformation, while peptides following the sequence pattern *cyclo*(-Pro-D-Xaa-Yaa-Pro-D-Xaa-Yaa-)-are found exclusively in a βVIb,βVIb conformation. The reason for that different conformational behavior must be assigned to the inversed chirality of the proline following residue, as the ψ_{i+2} torsion is mainly affected. In *cyclo*(-Pro-Gly-Ser-Pro-Gly-Ser-)[46] glycine seems to function as a residue in the D configuration.

The low solubility of c(PAAPAA) (0.5 mg in 0.4 ml DMSO) prevents the conformational analysis of the third conformation (23%), which probably represents an intermediate structure on the transition path between the all-*trans* and the two-*cis* conformation. Evidence for an asymmetric conformation is given by a complete signal set for all six residues in the NMR spectra and one H^{α} H^{α} ROE between a proline and a preceding alanine residue. At 300 K exchange peaks are observed correlating the asymmetric and the two-*cis* conformation, while exchange with the all-*trans* structure becomes de-

TABLE III. Main Chain Torsion Values* Defining the Different β Turn Types Within the Peptides Examined

Peptide	Residue	φ	ψ	Turn type, position
c(PAAPAA)	Pro[1]	−56	119	βII, $i+1$
all-*trans*	Ala[2]	57	30	βII, $i+2$
(vacuum)	Ala[3]	−155	163	
	Pro[4]	−58	113	βII, $i+1$
	Ala[5]	67	17	βII, $i+2$
	Ala[6]	−145	162	
c(PAAPAA)	Pro[1]	−76	−24	βVIa, $i+2$
two-*cis*	Ala[2]	−81	84	
(vacuum)	Ala[3]	−43	129	βVIa, $i+1$
	Pro[4]	−74	−27	βVIa, $i+2$
	Ala[5]	−81	85	
	Ala[6]	−42	129	βVIa, $i+1$
c(PAAPAA)	Pro[1]	−73	−32	βVIa, $i+2$
two-*cis*	Ala[2]	−76	97	
(solvent)	Ala[3]	−53	135	βVIa, $i+1$
	Pro[4]	−73	−32	βVIa, $i+2$
	Ala[5]	−73	86	
	Ala[6]	−39	130	βVIa, $i+1$
c(*PAAPAA*)	D-Pro[1]	57	−122	βII′, $i+1$
all-*trans*	Ala[2]	−71	−19	βII′, $i+2$
(vacuum)	Ala[3]	−113	101	
	D-Pro[4]	56	−119	βII′, $i+1$
	Ala[5]	−73	−17	βII′, $i+2$
	Ala[6]	−115	101	
c(RGDFPG)	Arg[1]	−147	135	
all-*trans*	Gly[2]	57	−119	βII′, $i+1$
(solvent)	Asp[3]	−79	−11	βII′, $i+2$
	Phe[4]	−119	149	
	Pro[5]	−50	117	βII, $i+1$
	Gly[6]	119	−60	βII, $i+2$
c(RGDFPG)	Arg[1]	−62	108	βII, $i+1$
cis	Gly[2]	76	−8	βII, $i+2$
(solvent)	Asp[3]	−149	112	
	Phe[4]	−47	129	βVIa, $i+1$
	Pro[5]	−90	7	βVIa, $i+2$
	Gly[6]	−93	−170	
c(RGDFPA)	Arg[1]	−168	112	
all-*trans*	Gly[2]	70	−110	βII′, $i+1$
(solvent)	Asp[3]	−71	−17	βII′, $i+2$
	Phe[4]	−104	147	
	Pro[5]	−47	−37	βI, $i+1$
	Ala[6]	−73	−32	βI, $i+2$
c(RGDFPA)	Arg[1]	−62	109	βII, $i+1$
cis	Gly[2]	96	−20	βII, $i+2$
(solvent)	Asp[3]	−145	85	
	Phe[4]	−40	128	βVIa, $i+1$
	Pro[5]	−75	−21	βVIa, $i+2$
	Ala[6]	−63	158	

*The main chain torsion values are taken from the structures shown in Figures 3, 4, 5, and 7, that are obtained by averaging over the last 60 ps of restrained MD simulations and energy minimizations.

tectable at 320 K. A similar effect is found for *cyclo* (-Pro-D-Gln-Val-Pro-D-Gln-Val-) and *cyclo*(-Pro-D-Gln-Leu-Pro-D-Gln-Leu-) that adopt an asymmetric conformation in D_2O. The second conformations are represented by two Val-Pro (Leu-Pro) *cis* peptide bonds and show C_2 symmetry.[55] The coexistence of a C_2 symmetric all-*trans* conformation and an asymmetric structure was described for c(PSGPSG)[43] where the asymmetric conformation is formed by a Gly-Pro *trans* and a Gly-Pro *cis* peptide bond.

Nevertheless, we have been able to determine two of three detected conformations of a sequential C_2 symmetric model peptide which adopts a symmetric all-*trans* conformation with proline residues in the $i + 1$ position of two βII turns and a second conformation with two Ala-Pro *cis* peptide bonds, where Pro is located in the $i + 2$ positions of two type VIa β turns.

In contrast to c(PAAPAA), the D-Pro containing peptide c(*PAAPAA*) is conformationally homogeneous; only the all-*trans* isomer is observed. Again the peptide adopts a C_2 symmetric conformation, confirmed by a single set of NMR resonances observed for the D-Pro-Ala-Ala unit. The temperature coefficients of the NH resonances of Ala^2/Ala^5 and Ala^3/Ala^6 are −7.0 and −1.0 ppb/K, respectively, and indicate the hydrogen bond pattern of a βII′,βII′ turn structure with both D-Pro residues in the $i + 1$ position of the turns. The same conformation was observed from the restrained MD simulations that fulfills the distance constraints with an average restraint violation of 12 pm.

The φ, ψ dihedrals of the D-Pro-Ala fragments defining the β turn coincide with the ideal values of a βII′ turn (Tables I and III). The hydrogen bonds between the residues Ala^3 and Ala^6 are observed for 97 and 98% of the 60 ps in vacuo simulation.

The inversion of L-Pro to D-Pro yields in conformational homogeneity, when c(PAAPAA) is compared to c(*PAAPAA*). In the D-Pro peptide the φ angle of Pro is restricted to values around +60° and therefore D-Pro can occupy only the $i + 1$ position of either a βI′ or a βII′ turn (Table I). The βII′,βII′ conformation for c(*PAAPAA*) is in agreement with the βII,βII turn arrangement identified for c(*PAA*-*PAA*), which is the enantiomer and shows a mirror image structure.[48] The preference of D-amino acids for the $i + 1$ position of type II′ β turns in cyclic hexapeptides has been well documented by several investigations from our group and others.[18,38,56]

The D-Pro containing peptide c(*PAAPAA*) obviously lacks the steric features that are responsible for the *cis*/*trans* isomerism observed for c(PAAPAA) and instead of a second conformation, with the amino acid sequence shifted within the common underlying two-turn structure, only the all-*trans* structure is found. This observation will be discussed on the basis of further -Xaa-Pro-Yaa- containing cyclic hexapeptides in the concluding part of the following chapter.

In another series of peptides, containing the similar Xaa-Pro-Yaa motif, comparable conformational

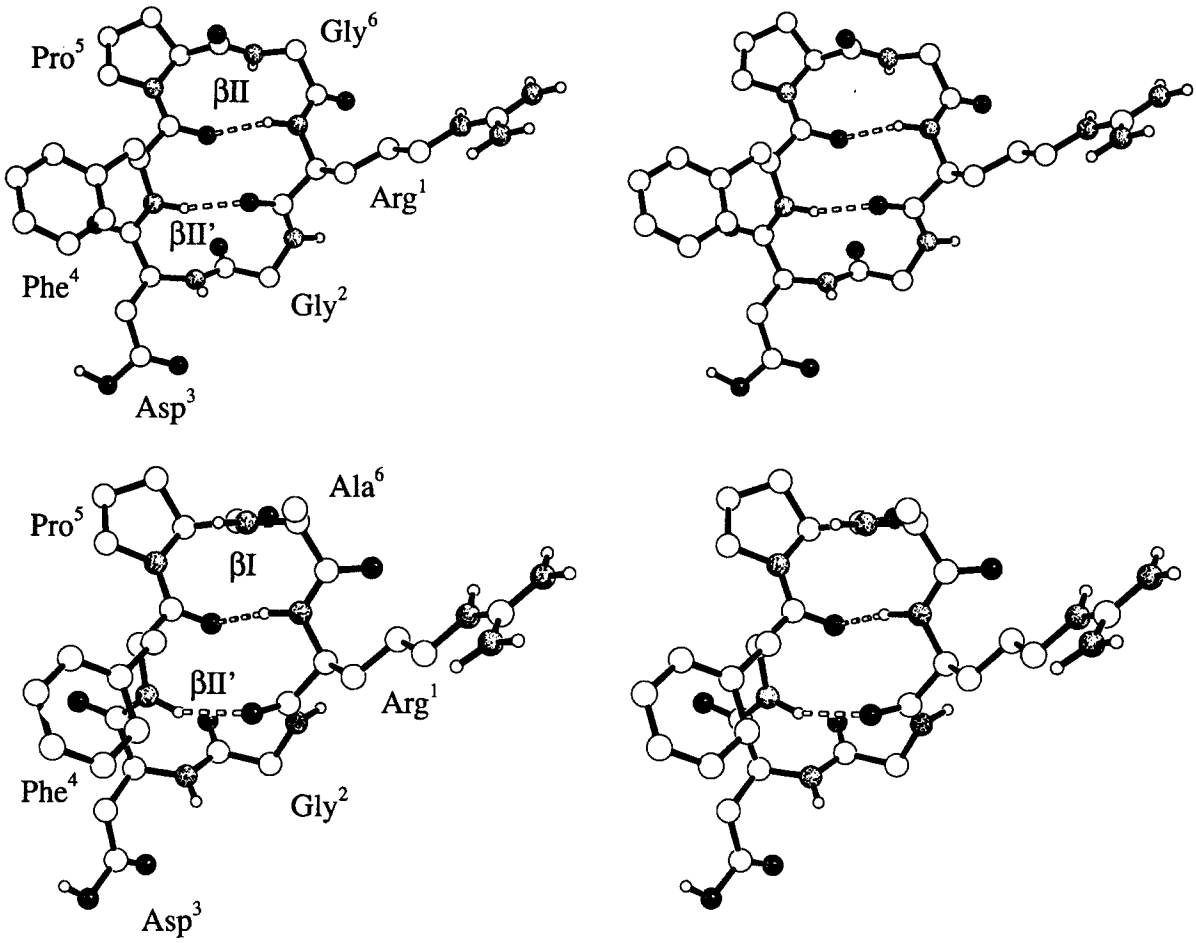

Fig. 4. Stereoplot of the all-trans conformations of c(RGDFPG) (**top**) and c(RGDFPA) (**bottom**). Oxygen atoms are depicted as filled balls, nitrogen atoms stippled, carbon atoms and hydrogen atoms are shown as plain balls. Hydrogen bonds are indicated as broken bonds.

features were expected. We will focus on the discussion of *cyclo*(-Arg^1-Gly^2-Asp^3-Phe^4-Pro^5-Gly^6-) and *cyclo*(-Arg^1-Gly^2-Asp^3-Phe^4-Pro^5-Ala^6-) and their corresponding D-Pro containing parent peptides. Both peptides are expected to adopt similar conformations because they only differ by a single methyl group at residue 6 (Gly→Ala). However, the *trans* conformation of c(RGDFPG) shows a βII,βII′ turn structure with Pro^5 in the $i + 1$ position of the βII turn and Gly^2 in the $i + 1$ position of the βII′ turn (Fig. 4, top), while c(RGDFPA) adopts a different conformation with a βI, βII′ turn structure (Fig. 4, bottom). In the latter peptide, a βI turn is formed with Pro^5 in the $i + 1$ position, and therefore the $i + 1$, $i + 2$ connecting amide bond is rotated by 180° when compared to the βII turn of c(RGDFPG) (Fig. 4). A comparable βII turn for the Ala^6 peptide is energetically unfavored because the C$^\beta$ atom of Ala in the $i + 2$ position would create steric conflicts with the carbonyl oxygen of the central amide bond. Therefore, the $i + 1$, $i + 2$ peptide bond is twisted by 180° to avoid the steric contact of Pro^{5}CO and Ala^{6}C$^\beta$. Interestingly, this generally accepted finding[10] is in contrast to the above discussed all-*trans* conformation of c(PAAPAA) that forms two βII turns with the sequence motif Pro^{i+1}-Ala^{i+2}. In the case of the RGD peptides, the introduction of a methyl group in position $i + 2$ of a β turn clearly favors the type I β turn. This is the only difference of the *trans* conformers of c(RGDFPG) and c(RGDFPA); the Arg^1-Gly^2-Asp^3-Phe^4 sequence forms the βII′ turn in both compounds with similar conformational features.

The temperature coefficients of Arg^{1}NH and Phe^{4}NH, −0.9 and −3.2 ppb/K, in the Gly^6 peptide as well as +3.0 ppb/K and −1.0 ppb/K in the Ala^6 peptide clearly support the stabilizing hydrogen bonds of the turn structures.

In the second conformation proline is shifted into the $i + 2$ position of a βVIa turn and a βII turn is formed with Arg^1 in $i + 1$ and Gly^2 in $i + 2$ position (Fig. 5).

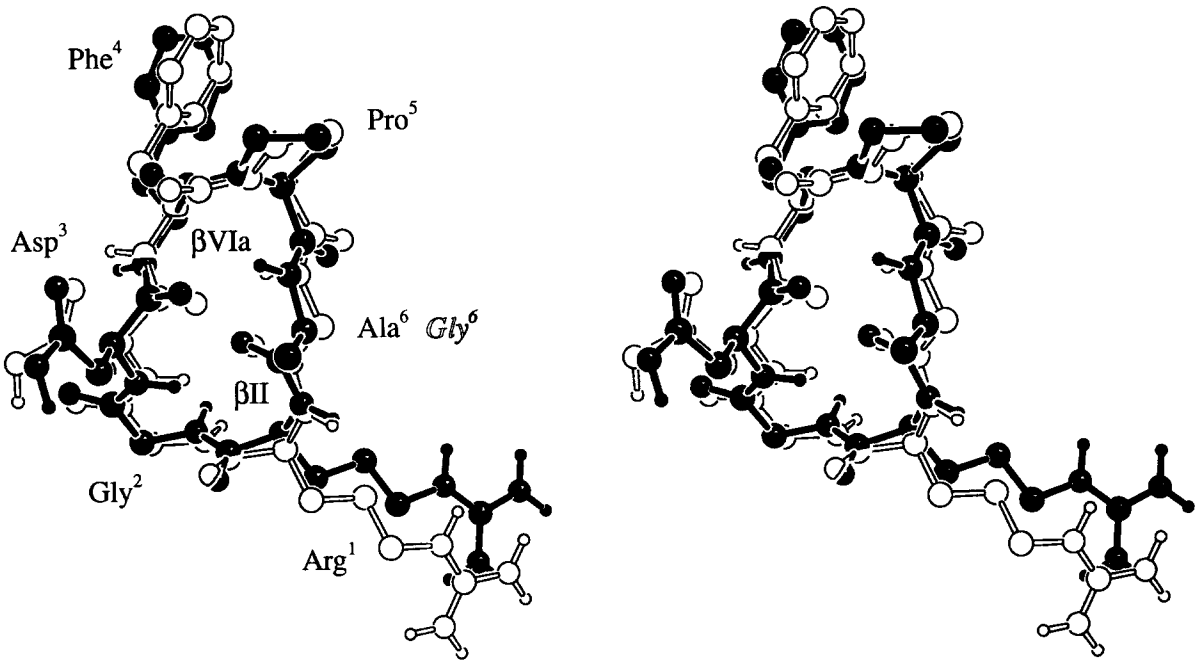

Fig. 5. Stereoplot of the superposition of the *cis* conformations of c(RGDFPG) (contours only) and c(RGDFPA) (filled black).

Again the temperature coefficients of the amide resonances are in accordance with the shifted hydrogen bonds in both peptides, formed between Gly^6 and Asp^3 and between Ala^6 and Asp^3 in c(RGDFPG) and c(RGDFPA), respectively. The values are in the range of 0.0 to −3.2 ppb/K, while the gradients of all other amide resonances are smaller than −4.0 ppb/K. The main chain torsion values of the turn forming residues Phe^4 and Pro^5 are in good agreement with the ideal torsion values as shown in Table III. The conformers of all RGD peptides discussed are refined by restrained MD simulations in solution; the experimentally derived distance constraints for the four structures are given in Table IV.

cis/trans Isomerism

The ratios of the *cis* and *trans* isomers of both RGD peptides c(RGDFPG) and c(RGDFPA) are of interest. For the Gly^6 peptide, the equilibrium is shifted in favor of the all-*trans* structure (71%). The introduction of a single methyl group in the $i + 2$ position of the βI turn of the all-*trans* peptide shifts the population to favor the βVIa turn containing *cis* conformation (75%). This observation is supported by the investigation of a further cyclic hexapeptide, published in 1989, with the sequence *cyclo*(-Phe^1-Pro^2-Thr^3-Lys^4-Trp^5-Phe^6-).[57] Again two conformations are observed, the major conformation is populated by 98% and contains a βVIa turn with a *cis* peptide bond between Phe^1 and Pro^2.

Here the more bulky side chain of Thr, a β branched amino acid, destabilizes a possible βI or βII turn with L-Pro^2 in the $i + 1$ position. Hence, we stress the importance of the degree of substitution of the residue following the proline for the stability of a βI or βII turn with proline in the $i + 1$ position on one hand, and the stability of a βVIa turn with proline in the $i + 2$ position on the other hand. *The higher the substitution of the residue following the proline, the more the equilibrium is shifted toward the* cis *conformation* as shown by the *cis/trans* ratios for the series -Phe-Pro-Gly- 29:71, -Phe-Pro-Ala- 75:25, -Phe-Pro-Thr- 98:2, although the latter peptide differs in the rest of the sequence.

Previously published work on the ratio of *cis/trans* isomers of proline containing cyclic hexapeptides pointed out that the ratio is solvent dependent[51] and further assigned the relief of steric hinderance between the side chain of an L-residue preceding proline and the CH_2^δ group of proline as a driving force favoring the *cis* conformation.[48] As all of the conformational investigations presented here were carried out in DMSO, we can rule out the solvent dependence as a possible parameter influencing the *cis/trans* ratio. Additionally, our reference molecules follow a common peptide fragment sequence with a conserved phenylalanine, -Phe-Pro-Xaa-, therefore the influence of the proline preceding residue on stability can be ruled out, too. Here, we investigate a further structural parameter on turn stabilization that is the steric demand of the sidechain of the proline-*following* residue, while all other variables like solvent properties and steric demand of proline preceding residues are kept constant and therefore are

TABLE IV. Comparison of Experimental (NOESY) and Calculated (MD) Interproton Distances of c(RGDFPG) and c(RGDFPA) in the all-*trans* and *cis* Conformation

Proton pair		r^{upper} (pm)	r^{lower} (pm)	r^{MD} (pm)
c(RGDFPG) *trans*				
Arg^1NH	Arg^1H^{α}	278	276	283
Arg^1NH	$Arg^1H_2^{\beta}$*	406	310	332
Arg^1NH	Pro^5H^{α}	380	360	403
Arg^1NH	$Gly^6H_2^{\alpha}$*	420	310	309
Arg^1H^{α}	$Arg^1H_2^{\beta}$*	334	240	269
Arg^1H^{α}	$Arg^1H_2^{\gamma}$*	384	285	254
Gly^2NH	$Gly^2H^{\alpha proS}$	270	244	275
Asp^3NH	Asp^3H^{α}	284	272	286
Asp^3NH	$Asp^3H_2^{\beta}$*	342	252	291
Asp^3NH	Phe^4NH	257	240	264
Asp^3H^{α}	$Asp^3H_2^{\beta}$*	339	249	277
Phe^4NH	Asp^3H^{α}	314	300	335
Phe^4NH	Phe^4H^{α}	266	264	290
Phe^4NH	$Phe^4H^{\beta proR}$	262	245	252
Phe^4NH	$Phe^4H^{\beta proS}$	336	308	372
Phe^4H^{α}	$Pro^5H_2^{\delta}$*	430	213	233
Phe^4H^{α}	$Phe^4H^{\beta proR}$	297	267	302
Phe^4H^{α}	$Phe^4H^{\beta proS}$	258	252	254
Pro^5H^{α}	$Pro^5H^{\beta proR}$	303	283	303
Pro^5H^{α}	$Pro^5H^{\beta proS}$	238	232	235
Gly^6NH	Arg^1NH	271	264	310
Gly^6NH	Pro^5H^{α}	215	206	207
Gly^6NH	$Pro^5H_2^{\beta}$*	438	314	387
Gly^6NH	$Gly^6H_2^{\alpha}$*	336	213	255
c(RGDFPA) *trans*				
Arg^1NH	Ala^6NH	300	277	279
Arg^1NH	Arg^1H^{α}	254	243	273
Arg^1H^{α}	$Arg^1H^{\beta proR}$	293	271	304
Arg^1H^{α}	$Arg^1H^{\beta proS}$	275	261	252
Gly^2NH	Arg^1H^{α}	218	214	215
Gly^2NH	$Gly^2H_2^{\alpha}$*	379	222	238
Asp^3NH	Asp^3H^{α}	287	266	281
Asp^3NH	$Asp^3H_2^{\beta}$*	330	240	299
Asp^3H^{α}	$Asp^3H_2^{\beta}$*	332	242	302
Phe^4NH	Asp^3NH	240	234	261
Phe^4NH	$Phe^4H^{\beta proR}$	235	229	237
Phe^4NH	$Phe^4H^{\beta proS}$	339	315	358
Phe^4H^{α}	$Pro^5H_2^{\delta}$*	303	208	226
Phe^4H^{α}	$Phe^4H^{\beta proR}$	305	282	303
Phe^4H^{α}	$Phe^4H^{\beta proS}$	263	245	248
Ala^6NH	$Phe^4H_2^{\beta}$*	405	315	325
Ala^6NH	Pro^5H^{α}	364	352	355
Ala^6NH	$Pro^5H^{\beta proR}$	254	251	261
Ala^6NH	$Pro^5H_2^{\delta}$*	427	307	367
Ala^6NH	Ala^6H^{α}	262	252	280
Ala^6NH	$Ala^6CH_3^{\beta}$	351	246	268
Arg^1NH	$Gly^6H^{\alpha proS}$	278	265	248
Arg^1NH	$Gly^6H^{\alpha proR}$	296	285	274
Arg^1NH	Arg^1H^{α}	285	275	275
Arg^1NH	$Arg^1H^{\beta proR}$	274	247	233
Arg^1NH	$Arg^1H^{\beta proS}$	319	290	353
Gly^2NH	Arg^1H^{α}	250	222	213
Gly^2NH	$Gly^2H^{\alpha proS}$	299	274	282
Gly^2NH	$Gly^2H^{\alpha proR}$	255	242	222
Gly^2NH	Asp^3NH	300	290	291
Asp^3NH	$Gly^2H^{\alpha proR}$	364	345	340
Asp^3NH	Asp^3H^{α}	295	285	289
Asp^3NH	$Asp^3H^{\beta proR}$	229	219	264
Asp^3NH	$Asp^3H^{\beta proS}$	332	312	319
Asp^3H^{α}	$Asp^3H^{\beta proR}$	268	248	299
Asp^3H^{α}	$Asp^3H^{\beta proS}$	236	227	238
Phe^4NH	Asp^3H^{α}	258	225	211
Phe^4NH	$Phe^4H^{\beta proR}$	273	261	229
Phe^4NH	$Phe^4H^{\beta proS}$	285	269	246
Phe^4H^{α}	$Phe^4H^{\beta proR}$	236	227	231
Phe^4H^{α}	$Phe^4H^{\beta proS}$	310	295	300
Gly^6NH	Phe^4H^{α}	310	300	298
Gly^6NH	$Gly^6H^{\alpha proS}$	238	221	234
Gly^6NH	$Gly^6H^{\alpha proR}$	289	259	293
c(RGDFPA) *cis*				
Arg^1NH	Ala^6H^{α}	244	238	245
Arg^1NH	$Ala^6CH_3^{\beta}$	365	256	333
Arg^1NH	Arg^1H^{α}	293	290	281
Arg^1NH	$Arg^1H_2^{\delta}$*	510	414	485
Gly^2NH	$Gly^2H_2^{\alpha}$*	334	213	248
Gly^2NH	Asp^3NH	275	264	286
Asp^3NH	$Gly^2H_2^{\alpha}$*	437	301	319
Asp^3NH	Asp^3H^{α}	291	286	292
Asp^3NH	$Asp^3H^{\beta proR}$	321	302	295
Asp^3NH	$Asp^3H^{\beta proS}$	342	324	322
Asp^3NH	$Ala^6CH_3^{\beta}$	429	333	410
Asp^3H^{α}	$Asp^3H_2^{\beta}$*	350	260	275
$Asp^3H_2^{\beta}$	$Ala^6CH_3^{\beta}$	418	287	449
Phe^4NH	Asp^3NH	333	324	346
Phe^4NH	Asp^3H^{α}	239	233	227
Phe^4NH	Phe^4H^{α}	284	276	267
Phe^4NH	$Phe^4H^{\beta proR}$	246	221	212
Phe^4NH	$Phe^4H^{\beta proS}$	257	251	249
Phe^4H^{α}	$Phe^4H_2^{\beta}$*	307	217	277
Pro^5H^{α}	$Pro^5H^{\beta proR}$	284	276	272
Pro^5H^{α}	$Pro^5H^{\beta proS}$	237	229	232
Ala^6NH	Phe^4H^{α}	271	268	303
Ala^6NH	$Pro^5H^{\beta proR}$	395	385	395
Ala^6NH	$Pro^5H_2^{\delta}$*	470	321	354
Ala^6NH	Ala^6H^{α}	282	281	285
Ala^6NH	$Ala^6CH_3^{\beta}$	356	254	268

*r^{upper} is increased by 90 pm due to the lack of diastereotopic assignment.

decoupled. We believe that such systematic studies of single structure variations are a powerful approach to understand the contributions of separate effects on turn stability.

We propose a possible contribution to the destabilization of a βI or βII turn with *trans* peptide bonds by a single structural variation. A direct comparison of a βII′ turn with D-Pro in the $i + 1$ position (Fig.

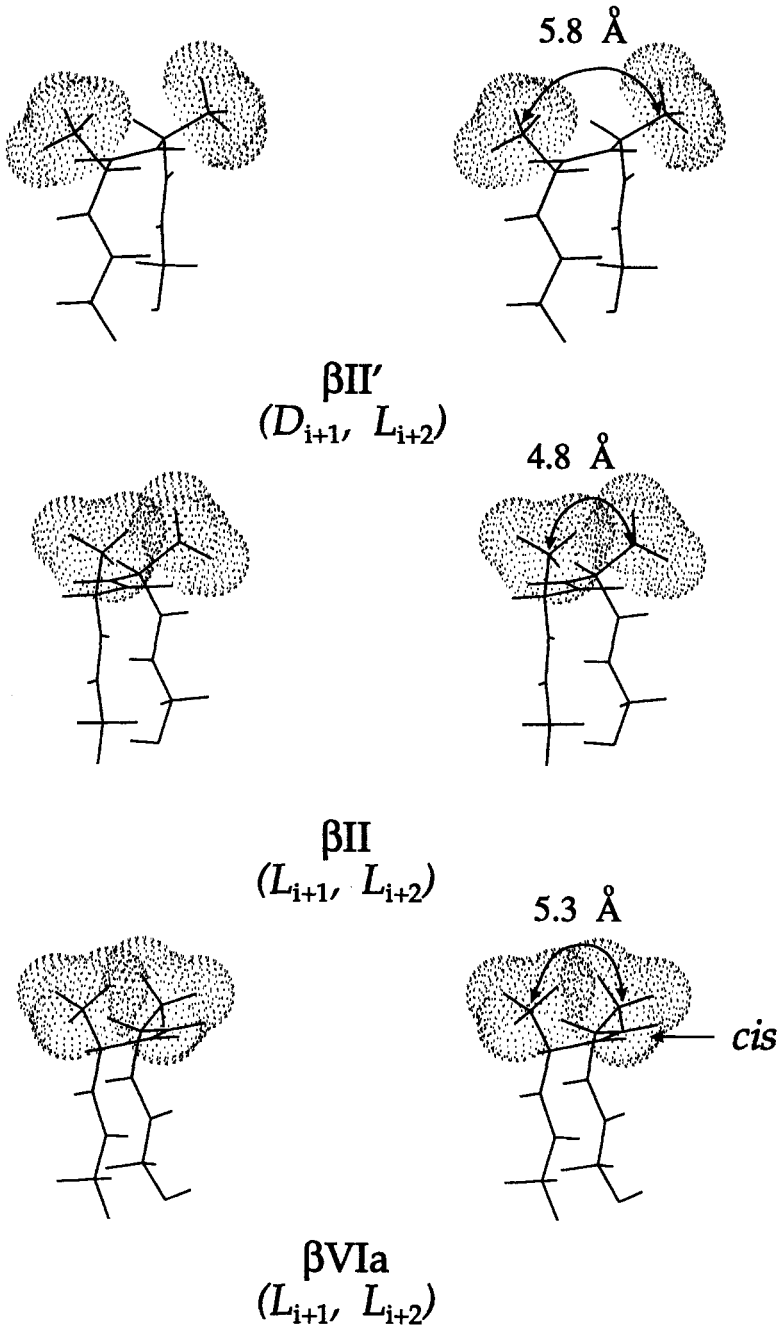

Fig. 6. Comparison of a βII' turn with a D-residue in $i + 1$ position (**top**), with a βII turn containing L-amino acids (**middle**), and a βVIa turn consisting of L-residues (**bottom**).

6, top), a βII turn with L-Pro in the $i + 1$ position (Fig. 6, middle), and a βVIa turn with L-Pro in the $i + 2$ position (Fig. 6, bottom) highlights some important short-range interactions.

In the βII' turn, the C^{β} atoms of residues $i + 1$ and $i + 2$ are arranged in a sort of *staggered* conformation, directed in opposite directions in reference to the peptide ring plane and are separated by 5.8 Å. With two L-residues in a βII turn the C^{β} atoms are exposed in a nearly parallel manner, so that they appear in an unfavored *eclipsed* conformation and the distance between them is decreased to 4.8 Å. This spatial proximity of the $i + 1$ and $i + 2$ C^{β} atoms together with the already mentioned $C^{\beta}{}_{i+2}$ CO_{i+1} steric contact leads to destabilization and therefore a conformational rearrangement of the cyclic hexapeptide occurs, with a shift of the sequence by one position, i.e., proline is displaced to the $i + 2$

TABLE V. Structural, Sequential and Conformational Characteristics of Selected βVI Turn Containing Proteins

Protein*	Pro^{x}_{i+2}	ϕ_{i+1}	ψ_{i+1}	ϕ_{i+2}	ψ_{i+2}	Type	Xaa_{i+1}	χ_1^{i+1}	Xaa_{i+3}
1ECA	74	−53	140	−101	24	βVIa	Leu	−61	Asn
1SBT	168	−98	145	−84	8	βVIa	Tyr	−65	Gly
2SNS	117	−100	114	−114	37	βVIa	Lys	−101	Leu
3TLN	51	−122	154	−79	−15	βVIa	Leu	−65	Gly
5RSA	93	−49	131	−85	2	βVIa	Tyr	−178	Asn
1HMQ	7A	−136	113	−61	154	βVIb	Asp	158	Tyr
	7B	−140	112	−66	148	βVIb	Asp	−161	Tyr
	7C	−141	112	−69	161	βVIb	Asp	−164	Tyr
	7D	−129	117	−69	161	βVIb	Asp	−160	Tyr
1OVO	12A	−106	164	−73	160	βVIb	Tyr	−67	Lys
	12B	−113	156	−76	165	βVIb	Tyr	−73	Lys
	12C	−118	153	−75	159	βVIb	Tyr	−66	Lys
	12D	−126	149	−76	157	βVIb	Tyr	−69	Lys
1PCY	16	−124	118	−66	163	βVIb	Val	−173	Ser
	36	−68	163	−79	157	βVIb	Phe	32	His
1REI	8a	−136	149	−64	−175	βVIb	Ser	−164	Ser
	8b	−151	148	−65	−176	βVIb	Ser	−166	Ser
	95a	−88	154	−56	149	βVIb	Leu	−54	Tyr
	95b	−74	148	−83	171	βVIb	Leu	−86	Tyr
1SN3	59	−67	126	−97	143	βVIb	Tyr	−171	Leu
2SGA	99	−165	140	−80	−151	βVIb	Phe	174	Asn
2TBV	359	−152	118	−92	118	βVIb	Leu	−80	Ala
3BCL	39	−136	155	−74	160	βVIb	Asn	−95	Thr
	320	−174	108	−64	147	βVIb	Ala	—	Ala
3FAB	h151	−175	145	−83	−177	βVIb	Phe	165	Glu
3GRS	375	−127	107	−74	168	βVIb	His	−60	Pro
	468	−124	146	−98	123	βVIb	His	−179	Thr
5RSA	114	−147	115	−62	153	βVIb	Asp	170	Tyr

*Taken from Brookhaven Protein Data Bank. 1ECA, hemoglobin (erythrocruorin)[65]; 1HMQ, hemerythrin[66]; 1OVO, ovomucoid third domain[67]; 1PCY, plastocyanin[68]; 1REI, Bence–Jones immunoglobulin[69]; 1SBT, subtilisin[70]; 1SN3, scorpion neurotoxin[63]; 2SGA, proeinase A[71]; 2SNS, staphylococcal nuclease[72]; 2TBV, tomato bushy stunt virus[73]; 3BCL, bacteriochlorophyll-A protein[74]; 3FAB, lambda immunoglobulin FAB′[75]; 3GRS, glutathione reductase[76]; 3TLN, thermolysin[77]; 5RSA, ribonuclease A.[64]

position of a βVIa turn. Due to the central *cis* configurated peptide bond preceding the proline, the C^{β} atom of residue $i + 1$ in the L-configuration is now arranged in a *staggered* conformation, similar in this regard to a D-residue in a βII′ turn. In this way the steric C^{β}_{i+1}, C^{β}_{i+2} conflict, which increases with the size of the side chain in the $i + 1$ position, is resolved by peptide bond isomerism together with a shift of the complete turn arrangement.

However, this model alone would not explain the destabilization of a type I β turn with all-*trans* peptide bonds and proline in the $i + 1$ position. Here, the C^{β}_{i+1}, C^{β}_{i+2} distance is around 5.3 Å and therefore is not increased when the peptide sequence shifts clockwise to a βVIa turn structure. Nevertheless, the spatial demand of the proline-following residue correlates with the increasing population of the *cis* conformation and reflects the importance of the substitution pattern of turn regions.

Further support for the idea of the C^{β}_{i+1}, C^{β}_{i+2} destabilizing interaction is the finding that all related D-Pro containing peptides investigated here, c(*PAAPAA*), c(RGDF*PG*), and c(RGDF*PA*), adopt one conformation exclusively with all-*trans* peptide bonds with D-Pro in the $i + 1$ position of well defined type II′ β turns.

To expand the study to protein structures, a search for β VI turns was carried out. Five βVIa turn containing proteins, available from the Brookhaven Protein Data Bank (Table V) were analyzed.

Three of the proteins bear highly substituted side chains at their $i + 3$ residues of the βVIa turns, as would be predicted from our results. However, the remaining two have a Gly in the $i + 3$ position which may demonstrate the importance of the protein environment for turn stability. Within globular structures the sum of a wide variety of interactions determines the stability and conformation of the surface loops. This complexity makes it difficult to analyze single effects responsible for a certain loop structure. In addition with only five examples of high resolution X-ray structures of β VIa turn-containing proteins it is not possible to draw statistically reliable conclusions. Nevertheless, three of the five analyzed turns (1ECA, 2SNS, 5RSA) are in accordance with the structural requirements obtained from our peptide studies.

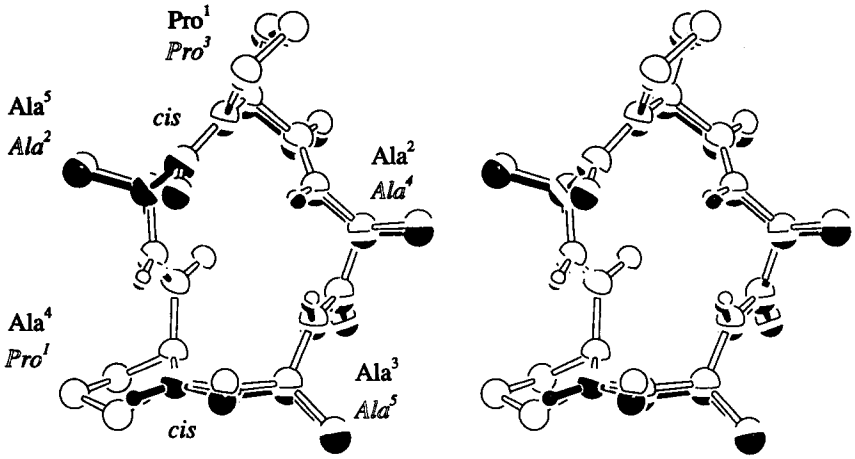

Fig. 7. Stereoplot of the superposition of the major conformation of c(PAAAA) (filled black) and c(PAPAA) (contours only); both *cis* peptide bonds are assigned.

βVIb Peptides

We will focus now on the conformational discussion of two βVIb turn-containing model peptides, c(PAAAA) and a more constrained analogue c(PAPAA). While c(PAPAA) adopts a single conformation, the less restricted Ala³ analogue c(PAAAA) adopts at least three different conformations. Two of them are populated by less than 10% so that only the major conformation could be analyzed. All structural relevant parameters of the major conformation of c(PAAAA) are nearly identical to c(PAPAA), counting for a similar structure. Two *cis* peptide bonds are indicated by the already mentioned difference of the ^{13}C chemical shift values of Pro C^{β} and C^{γ} in the range of 10 ppm (Table II) and the intensive ROE effects correlating the H^{α} resonances of two subsequent residues. Interestingly in c(PAAAA) two Ala residues form a *cis* peptide bond, confirmed by a short distance of 210 pm between Ala^3H^{α} and Ala^4H^{α} (Fig. 7, black) which is rather unusual for peptides. The restrained MD simulations were carried out with 19 and 23 distance constraints for c(PAAAA) and c(PAPAA), respectively, and average restrained violations of 8 and 7 pm have been achieved.

The dihedral angles from the restrained MD simulations indicate that both *cis* peptide bonds are in the central part ($i + 1, i + 2$) of two *intertwined* type VIb β turns (Table VI, Fig. 7).

The derived conformations of the peptides are nearly identical, indicated by a rms deviation for superposition of the peptide backbone atoms of only 0.09 Å. Three of the four βVIb turns discussed here contain a proline residue in the $i + 2$ position and in the case of c(PAAAA) the sequence Ala^2_i-Ala^3_{i+1}-Ala^4_{i+2}-Ala^5_{i+3} forms a type VIb β turn. The characterizing dihedrals of the amino acids in position $i + 1$ and $i + 2$ coincide with the ideal

TABLE VI. Main Chain Torsion Values of c(PAAAA) and c(PAPAA)

Residue	ϕ	ψ	ω	Turn type*
		c(PAAAA)		
Pro^1	−82	−2	−179	*i*+2 βVIb
Ala^2	−118	−55	179	
Ala^3	−140	90	−12	*i*+1 βVIb
Ala^4	−83	−28	−178	*i*+2 βVIb
Ala^5	−122	125	−11	*i*+1 βVIb
		c(PAPAA)		
Pro^1	−76	−28	−177	*i*+2 βVIb
Ala^2	−126	127	−9	*i*+1 βVIb
Pro^3	−82	2	−178	*i*+2 βVIb
Ala^4	−123	−56	178	
Ala^5	−140	69	−18	*i*+1 βVIb

*Corresponding turns in both structures are indicated by the same type of print (italics, normal).

values found in the literature.[5,9,10] Nevertheless, the comparison of βVI turn geometries in crystallographically refined protein structures with the defined ideal values results in a significant deviation for the ψ_{i+2} torsion value. In all examined proteins (Table VI), ψ_{i+2} adopts a value of about +150°, which is in accordance with a recently published investigation by Richardson and Richardson.[58] This value, in contrast to the standard value of 0°, directs the $i + 2$ carbonyl oxygen into the interior of the turn and, therefore, no stabilizing hydrogen bond can be formed (Fig. 8).

This finding is supported by the previously published C_2 symmetric peptides adopting a βVIb,βVIb conformation in their two-*cis* structure.[46,47,51,54] The ψ angle of proline is found at values around 150°.

Hence, we find a contradiction in the literature between the definition of the torsion values characterizing the turn and the structural results found for

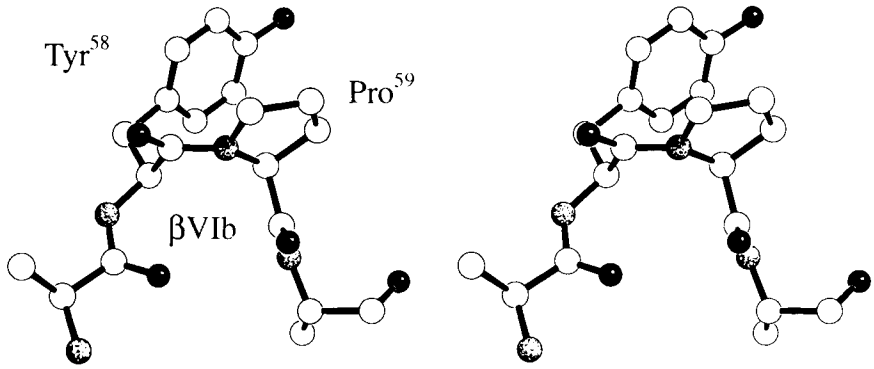

Fig. 8. A βVIb turn formed by the residues Thr[57]-Tyr[58]-Pro[59]-Leu[60] of scorpion neurotoxin (1SN3).[61]

βVIb turns in proteins concerning the value of ψ_{i+2}.[9,59,60]

Examining the βVI turns of the analyzed proteins (Table IV), a sequential preference of hydrophobic or aromatic amino acids in position $i + 1$ is found, as previously described by Richardson and Richardson.[58] A more detailed analysis of the side chain orientations of the aromatic $i + 1$ residues using homo- and heteronuclear coupling constants results in a preferred value of about 180° for χ_1. In all of the -Phe-Pro-Yaa- containing cyclic hexapeptides investigated here, the side chain of Phe is found exclusively in a 180° orientation (Figs. 5, 8, and 9). This particular exposition of the aromatic side chain allows a parallel alignment of the phenyl ring plane relative to the proline ring. Further evidence for the proximity of both rings are the chemical shift values of the proline H^{α} resonances which show an unusual highfield shift: 3.02 for c(FPTKWF), 2.83 for c(RGDFPG), and 3.02 for c(RGDFPA). In addition the highfield shifted resonances of proline $H^{\beta proR}$ at 1.00 ppm counts for a position of that proton pointing toward the plane of the phenylalanine ring. These spectroscopic effects can be explained by the anisotropic shift effect of the phenyl ring that shields the affected proline hydrogen atoms. A further support for that preferred side chain rotamer is derived from the X-ray structure of *cyclo*(-Pro-D-Ala-Phe-Pro-D-Ala-Phe-)[54] where in all βVI turns the values of χ_1(Phe) are found between 173° and 178°. As a driving force for that turn conformation, we propose the existence of hydrophobic interactions between the phenyl ring and the proline ring. Normally, loop regions in proteins are exposed to solvent and generally contain charged and hydrophilic residues that can form hydrogen bonds to surrounding solvent molecules. In nearly all βVI turns, proline and a hydrophobic amino acid in the $i + 1$ position are exposed on the protein surface. To minimize the hydrophobic surface area of these nonpolar turn fragments the folding of an aromatic ring over the proline is favored, for it allows an attractive hydrophobic contribution to stability (Fig. 9).

CONCLUSION

We have developed a straightforward strategy to design β turn-containing cyclic peptides. The incorporation of appropriate residues, especially proline, and the variation of ring size enabled us to design compounds containing βVI turns, which are rather uncommon turns in native proteins. The peptides examined mimic the turn geometry found in crystallographically refined proteins at such a detailed level that even the preference of side chain orientations is reproduced. Comparing our results with βVI turns of proteins we have proposed an explanation for the sequential preference of aromatic residues in the $i + 1$ position of type VI β turns on the basis of NMR-derived experimental observations. In the case of peptides with *cis* and *trans* isomers, the ratio of the isomers depends on the extent of substitution of the residues following the proline, verified by examining a series of -Phe-Pro-Yaa- peptides.

Therefore, we studied a single intrinsic effect which is the steric demand of the proline-following residue while reducing the high dimensionality of all possible contributions to turn stability. We imagine this as an important result which has to be considered in designing turn structures containing proline. Further, we have shown that cyclic oligopeptides are excellent models to study conformational features of protein reverse turns, often responsible for molecular recognition processes, as we have demonstrated by the employment of a rational design of model compounds to biological relevant RGD peptides.[17,61,62] The results presented here will be of importance in understanding side chain interactions in loop structures within native proteins that stabilize preferred turn conformations.

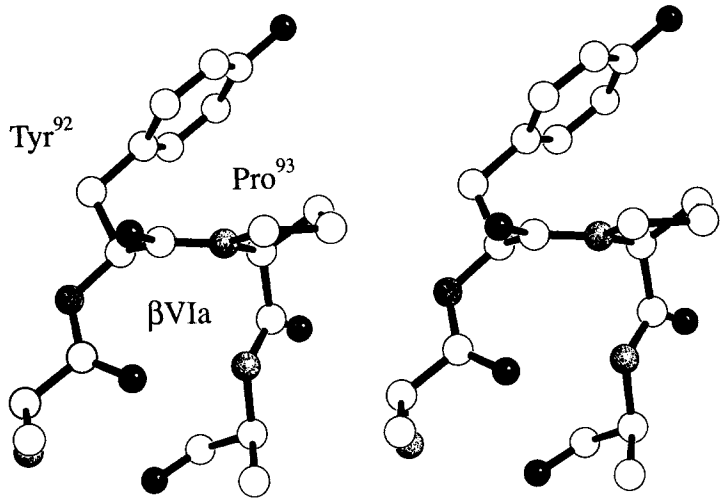

Fig. 9. Stereodrawing of the βVIa turn from ribonuclease A (5RSA) (EC 3.1.27.5).[62] The residues Cys[91]-Tyr[92]-Pro[93]-Asn[94] are part of the type VIa β turn.

ACKNOWLEDGMENTS

Financial support by the Fonds der Chemischen Industrie and the Deutsche Forschungsgemeinschaft is greatfully acknowledged. The authors thank the Studienstiftung des deutschen Volkes (M. Gurrath) and the Fonds der Chemischen Industrie (G. Müller) for doctoral fellowships and Dr. Dale F. Mierke for carefully reading the manuscript.

REFERENCES

1. Pauling, L., Corey, R. B., Branson, H. R. The structure of proteins: Two hydrogen-bonded helical configurations of the polypeptide chain. Proc. Natl. Acad. Sci. U.S.A. 37: 205–211, 1951.
2. Braut, D. A. Conformational energy estimates for helical polypeptide molecules. Macromolecules 1:291–300, 1968.
3. Hol, W. G. J., van Duijnen, P. T., Berendsen, H. J. C. The α-helix dipole and the properties of proteins. Nature (London) 273:443–446, 1978.
4. Richardson, J. S. The anatomy and taxonomy of protein structure. Adv. Protein Chem. 34:167–339, 1981.
5. Milner-White, E. J., Poet, R., Loops, bulges, turns and hairpins in proteins. Trends Biochem. Sci. 12:189–192, 1987.
6. Sibanda, B. L., Thornton, J. M. β-Hairpin families in globular proteins. Nature (London) 316:170–174, 1985.
7. Venkatachalam, M. Stereochemical criteria for polypeptides and proteins: Conformation of a system of three linked peptide units. Biopolymers 6:1425–1436, 1968.
8. Lewis, P. N., Momany, F. A., Scheraga, H. A. Chain reversals in proteins. Biochem. Biophys. Acta 303:211–229, 1973.
9. Rose, G. D., Gierasch, L. M., Smith, J. A. Turns in peptides and proteins. Adv. Protein Chem. 37:1–109, 1985.
10. Smith, J. A., Pease, L. G. Reverse turns in peptides and proteins. CRC Crit. Rev. Biochem. 8:315–399, 1980.
11. Chou, P., Fasman, G. β turns in proteins. J. Mol. Biol. 115:135–175, 1977.
12. Blout, E. R. Why cyclic peptides? Complementary approaches to conformations. Acc. Chem. Res. 9:106–113, 1976.
13. Kessler, H., Gehrke, M., Griesinger, C. Two-dimensional NMR spectroscopy: Background and overview of the experiments. Angew, Chem. Int. Ed. Engl. 27:490–536, 1988.
14. Kessler, H. Conformation and biological activity of cyclic peptides. Angew. Chem. Int. Ed. Engl. 21:512–523, 1982.
15. Kessler, H. Peptide engineering: Design of biologically active peptides under conformational control. In: "Trends in Drug Research." Edited by Claasen, V. ed. Amsterdam: Elsevier Science Publishers, 1990:73–84.
16. D'Souza, S. E., Ginsberg, M. H., Plow, E. F. Arginyl-glycyl-aspartic acid (RGD): A cell adhesion motif. Trends Biochem. Sci. 16:246–250, 1991.
17. Aumailley, M., Gurrath, M., Müller, G., Calvete, J., Timpl, R., Kessler, H. Arg-Gly-Asp constrained within cyclic pentapeptides. Strong and selective inhibition of cell adhesion to vitronectin and laminin fragment P1. FEBS Lett. 291(1):50–54, 1991.
18. Bean, J. W., Kopple, K. D., Peishoff, C. E. Conformational analysis of cyclic hexapeptides containing the D-Pro-L-Pro sequence to fix β-turn positions. J. Am. Chem. Soc. 114: 5328–5334, 1992.
19. Piantini, U., Sørensen, O. W., Ernst, R. R. Multiple quantum filters for elucidating NMR coupling networks. J. Am. Chem. Soc. 104:6800–6801, 1982.
20. Braunschweiler, L., Ernst, R. R. Coherence transfer by isotropic mixing: Application to proton correlation spectroscopy. J. Magn. Reson. 53:521–528, 1983.
21. Bax, A., Byrd, R. A., Aszalos, A. Spin multiplet enhancement in two dimensional correlated NMR spectroscopy. J. Am. Chem. Soc. 106:7632–7633, 1984.
22. Wüthrich, K. "NMR of Proteins and Nucleic Acids." New York: John Wiley, 1986.
23. Neuhaus, D., Williams, M. P. "The Nuclear Overhauser Effect in Structural and Conformational Analysis." Cambridge, UK: VCH, 1989.
24. Bothner-By, A. A., Stephensen, R. L., Lee, J., Warren, C. D., Jeanloz, R. W. Structure determination of a tetrasaccharide: Transient nuclear Overhauser effect in the rotating frame. J. Am. Chem. Soc. 106:811–813, 1984.
25. Bax, A., Davis, D. G. Practical aspects of two-dimensional transverse NOE spectroscopy. J. Magn. Reson. 63:207–213, 1985.
26. Kessler, H., Griesinger, C., Kerssebaum, R., Wagner, K., Ernst, R. R. Separation of cross-relaxation and *J* cross-peaks in 2D rotating-frame NMR spectroscopy. J. Am. Chem. Soc. 109:607–609, 1987.
27. Kessler, H., Schmieder, P., Köck, M., Kurz, M. Improved resolution in proton-detected heteronuclear long-range correlation. J. Magn. Reson. 88:615–618, 1990.
28. Bermel, W., Griesinger, C., Wagner, K. Proton detected C,H correlation via long-range couplings with soft pulses; determination of coupling constants. J. Magn. Reson. 83: 223–232, 1989.
29. Kessler, H., Griesinger, C., Wagner, K. Peptide Conformations. 42. Conformation of side chains in peptides using heteronuclear coupling constants obtained by two-dimen-

sional NMR spectroscopy. J. Am. Chem. Soc. 109:6927–6933, 1987.
30. Müller, L. Sensitivity enhanced detection of weak nuclei using heteronuclear multiple quantum coherence. J. Am. Chem. Soc. 101:4481–4484, 1979.
31. Lerner, L., Bax, A. Sensitivity-enhanced two-dimensional heteronuclear relayed coherence transfer NMR spectroscopy. J. Magn. Reson. 69:375–380, 1986.
32. Kurz, M., Schmieder, P., Kessler, H. HETLOC, an efficient method for determining heteronuclear long-range couplings with heteronuclei in natural abundance. Angew. Chem. Int. Ed. Engl. 30:1329–1331, 1991.
33. Schmieder, P., Kurz, M., Kessler, H. Determination of heteronuclear long-range couplings to heteronuclei in natural abundance by two- and three-dimensional NMR spectroscopy. J. Biomol. NMR 1:403–420, 1991.
34. Griesinger, C., Ernst, R. R. Frequency offset effects and their elimination in NMR rotating-frame cross-relaxation spectroscopy. J. Magn. Reson. 75:261–271, 1987.
35. van Gunsteren, W. F., Berendsen, H. J. C. In GROMOS, Groningen Molecular Simulation (GROMOS) Library Manual, Nijenborgh, the Netherlands, 1–227, 1987.
36. van Gunsteren, W. F., Berendsen, H. J. C. Computer simulation of molecular dynamics: Methodology, applications and perspectives in chemistry. Angew. Chem. Int. Ed. Engl. 29:992–1023, 1990.
37. DISCOVER and INSIGHT II are commercially available from Biosym Technologies Inc., 10065 Barnes Canyon Rd, San Diego, CA 92121.
38. van Gunsteren, W. F., Berendsen, H. J. C. Algorithms for macromolecular dynamics and constrained dynamics. Mol. Phys. 34:1311–1327, 1977.
39. Mierke, D. F., Kessler, H. Molecular dynamics with dimethylsulfoxide as a solvent. Conformation of a cyclic hexapeptide. J. Am. Chem. Soc. 113:9466–9470, 1991.
40. Kessler, H., Bats, J. W., Griesinger, C., Koll, S., Will, M., Wagner, K. Peptide conformation. 46. Conformational analysis of a superpotent cytoprotective cyclic somatostatin analogue. J. Am. Chem. Soc. 110:1033–1049, 1988.
41. Kessler, H., Matter, H., Gemmecker, G., Kling, A., Kottenhahn, H. Solution structure of a synthetic N-glycosilated cyclic hexapeptide determined by NMR spectroscopy and MD calculations. J. Am. Chem. Soc. 113:7550–7563, 1991.
42. Stradley, S. J., Rizo, J., Bruch, M. D., Stroup, A. N., Gierasch, L. M. Cyclic pentapeptides as models for reverse turns: Determination of the equilibrium distribution between type I and type II conformations of Pro-Asn and Pro-Ala β-turns. Biopolymers 29:263–287, 1990.
43. Torchia, D. A., Corato, A. di, Wong, S. C. K., Deber, C. M., Blout, E. R. Cyclic peptides. II. Solution conformations of *cyclo*(prolylserylglycylprolylserylglycyl) from nuclear magnetic resonance. J. Am. Chem. Soc. 94:609–615, 1972.
44. Pease, L. G., Deber, C. M., Blout, E. R. Cyclic peptides. V. ^{1}H and ^{13}C nuclear magnetic resonance determination of the preferred β conformation for proline-containing cyclic hexapeptides. J. Am. Chem. Soc. 95:258–260, 1973.
45. Kostansek, E. C., Thiessen, W. E., Schomburg, D., Lipscomb, W. N. Crystal structure and molecular conformation of the cyclic hexapeptide *cyclo*-(Gly-L-Pro-Gly)$_2$. J. Am. Chem. Soc. 101:5811–5815, 1979.
46. Torchia, D. A., Wong, S. C. K., Deber, C. M., Blout, E. R. Cyclic peptides. III. Solution conformations of *cyclo*(serylprolylglycylserylprolylglycyl) from nuclear magnetic resonance. J. Am. Chem. Soc. 94:616–620, 1972.
47. Sarkar, S. K., Torchia, D. A., Kopple, K. D., VanderHart, D. L. Study of proline peptide bond conformation and ring dynamics in crystalline cyclic peptides using ^{13}C MAS NMR. J. Am. Chem. Soc. 106:3328–3331, 1984.
48. Gierasch, L. M., Deber, C. M., Madison, V., Niu, C.-H., Blout, E. R. Conformations of (X-L-Pro-Y)$_2$ cyclic hexapeptides. Preferred β-turn conformers and implications for β turns in proteins. Biochemistry 20:4730–4738, 1981.
49. Brown, J. N., Yang, C. H. Crystal and molecular structure of the cyclic hexapeptide *cyclo*-(Gly-Pro-*d*-Phe)$_2$. J. Am. Chem. Soc. 101:445–449, 1979.
50. Kostansek, E. C., Lipscomb, W. N., Thiessen, W. E. Crystal structure and conformation of the cyclic hexapeptide *cyclo*-(Gly-L-Pro-D-Ala)$_2$. J. Am. Chem. Soc. 101:834–837, 1979.
51. Kopple, K. D., Schamper, T. J., Go, A. Conformation of cyclic peptides. VIII. Cyclic hexapeptides containing the L-Pro-D-Phe sequence. J. Am. Chem. Soc. 96:2597–2605, 1974.
52. Brown, J. N., Teller, R. G. Crystal structure and molecular conformation of the hydrated cyclic hexapeptide *cyclo*(L-Ala-L-Pro-D-Phe)$_2$. J. Am. Chem. Soc. 98:7565–7569, 1976.
53. Kurz, M., Mierke, D. F., Kessler, H. Calculation of molecular dynamics for peptides in dimethyl sulfoxide: Elimination of vacuum effects. Angew. Chem. Int. Ed. Engl. 31: 210–212, 1992.
54. Kartha, G., Krishna Bhandary, K., Kopple, K. D., Go, A., Zhu, P.-P. Synthesis and conformational studies by X-ray crystallography and nuclear magnetic resonance of *cyclo*(L-Phe-L-Pro-D-Ala)$_2$. J. Am. Chem. Soc. 106:3844–3850, 1984.
55. Kopple, K. D., Parameswaran, K. N. Synthesis and backbone conformations of cyclic hexapeptides cyclo-(Xxx-Pro-D-Gln)$_2$. Int. J. Peptide Protein Res. 21:269–280, 1983.
56. Flippen-Anderson, J. L. Conformation of the cyclic hexapeptide (D-Phe-Pro-Val)$_2$: $C_{38}H_{50}N_6O_6$. In: "Peptides, Structure and Biological Function, Proceedings of the 6th American Peptide Symposium." Pierce Chemical Co., Rockford, IL: Washington, D. C., 1979:145–148.
57. Hofmann, M., Gehrke, M., Bermel, W., Kessler, H. Proton-detected C,H correlation NMR techniques for the complete assignment of all proton and carbon resonances of a cyclic peptide. Magn. Reson. Chem. 27:877–886, 1989.
58. Richardson, J. S., Richardson, D. C. Principles and patterns of protein conformation. In: "Prediction of Protein Structure and the Principles of Protein Conformation." Edited by Fasman, G. D. (ed.). New York: Plenum Press, 1989:1–98.
59. Wilmot, C. M., Thornton, J. M. Analysis and prediction of the different types of β turns in proteins. J. Mol. Biol. 203:221–232, 1988.
60. Wilmot, C. M., Thornton, J. M. β turns and their distortions: A proposed new nomenclature. Protein Eng. 3(6): 479–493, 1990.
61. Adler, M., Lazarus, R. A., Dennis, M. A., Wagner, G. Solution structure of Kistrin, a potent platelet aggregation inhibitor and gpIIb-IIIa antagonist. Science 253:445–448, 1991.
62. Saudek, V., Atkinson, R. A., Pelton, J. T. Three-dimensional structure of Echistatin, the smallest active RGD protein. Biochemistry 30:7369–7372, 1991.
63. Almassy, R. J., Fontecilla-Camps, J. C., Suddath, F. L., Bugg, C. E. Structure of variant-3 scorpion neurotoxin from Centruroides sculpturatus Ewing, refined at 1.8 Å resolution. J. Mol. Biol. 170:497–527, 1983.
64. Wlodawer, A., Sjolin, L. Structure of ribonuclease A. Results of joint neutron and x-ray refinement at 2.0 Å resolution. Biochemistry 22:2720–2728, 1983.
65. Steigemann, W., Weber, E. Structure of erythrocruorin in different ligand states refined at 1.4 Å resolution. J. Mol. Biol. 127:309–338, 1979.
66. Stenkamp, R. E., Sieker, L. C., Larry, C., Jensen, L. H. Adjustment of restraints in the refinement of methemerythrin and azidomethemerythrine at 2.0 Å resolution. Acta Crystallogr., Sect. B: Struct. Sci. B39:697–703, 1983.
67. Papamokos, E., Weber, E., Bode, W., Huber, R., Empie, M. W., Kato, I., Laskowski, M., Jr. Crystallographic refinement of Japanese quail ovomucoid, a Kazal-type inhibitor, and model building studies of complexes with serine proteases. J. Mol. Biol. 158:515–537, 1982.
68. Colman, P. M., Freeman, H. C., Guss, J. M., Murata, M., Norris, V. A., Ramshaw, J. A. M., Venkatappa, M. P. X-ray crystal structure analysis of plastocyanin at 2.7 Å resolution. Nature (London) 227:319–324, 1978.
69. Epp, O., Lattman, E. E., Schiffer, M., Huber, R., Palm, W. Molecular structure of a dimer composed of the variable portions of the Bence-Jones protein REI refined at 2.0 Å resolution. Biochemistry 14:4943–4952, 1975.
70. Wright, C. S., Alden, R. A., Kraut, J. Structure of subtilisin BPN' at 2.5 Å resolution. Nature (London) 221:235–242, 1969.
71. James, N. M. G., Sielecki, A. R., Brayer, G. D., Delbaere, L. T. J., Bauer, C. A. Structures of product and inhibitor complexes of Streptomyces griseus protease A of 1.8 Å resolution. A model for serine protease catalysis. J. Mol. Biol. 144:43–88, 1980.
72. Cotton, F. A., Hazen, E. E., Jr., Legg, M. J. Staphylococcal

nuclease: Proposed mechanism of action based on structure of enzyme-thymidine 3′,5′-bisphosphate-calcium ion complex at 1.5 Å resolution. Proc. Natl. Acad. Sci. U.S.A. 76:2551–2555, 1979.
73. Hopper, P., Harrison, S. C., Sauer, R. T. Structure of tomato bushy stunt virus. V. Coat protein sequence determination and its structural implications. J. Mol. Biol. 177: 701–713, 1984.
74. Tronrud, D. E., Schmid, M. F., Matthews, B. W. Structure and x-ray amino acid sequence of a bacteriochlorophyll a protein from Prosthecochloris aestuarii refined at 1.9 Å resolution. J. Mol. Biol. 188:443–454, 1986.
75. Saul, F., Amzel, L. M., Poljak, R. J. Preliminary refinement and structural analysis of the Fab fragment from human immunoglobulin New at 2.0 Å resolution. J. Biol. Chem. 253:585–597, 1978.
76. Karplus, P. A., Schulz, G. E. Refined structure of glutathione reductase at 1.54 Å. J. Mol. Biol. 195:701–729, 1987.
77. Holmes, M. A., Matthews, B. W. Structure of thermolysin refined at 1.6 Å resolution. J. Mol. Biol. 160:623–639, 1982.